0022-3565/10/3341-310–317$20.00
THE JOURNAL OF PHARMACOLOGY AND EXPERIMENTAL THERAPEUTICS
Copyright © 2010 by The American Society for Pharmacology and Experimental Therapeutics
JPET 334:310–317, 2010

Vol. 334, No. 1
165845/3599124
Printed in U.S.A.

A Novel Autotaxin Inhibitor Reduces Lysophosphatidic Acid Levels in Plasma and the Site of Inflammation[S]

James Gierse, Atli Thorarensen, Konstantine Beltey, Erica Bradshaw-Pierce, Luz Cortes-Burgos, Troii Hall, Amy Johnston, Michael Murphy, Olga Nemirovskiy, Shinji Ogawa, Lyle Pegg, Matthew Pelc, Michael Prinsen, Mark Schnute, Jay Wendling, Steve Wene, Robin Weinberg, Arthur Wittwer, Ben Zweifel, and Jaime Masferrer

Pfizer Inflammation Research, Chesterfield, Missouri

Received January 11, 2010; accepted April 13, 2010

ABSTRACT

Autotaxin is the enzyme responsible for the production of lysophosphatidic acid (LPA) from lysophosphatidyl choline (LPC), and it is up-regulated in many inflammatory conditions, including but not limited to cancer, arthritis, and multiple sclerosis. LPA signaling causes angiogenesis, mitosis, cell proliferation, and cytokine secretion. Inhibition of autotaxin may have anti-inflammatory properties in a variety of diseases; however, this hypothesis has not been tested pharmacologically because of the lack of potent inhibitors. Here, we report the development of a potent autotaxin inhibitor, PF-8380 [6-(3-(piperazin-1-yl)propanoyl)-benzo[d]oxazol-2(3*H*)-one] with an IC_{50} of 2.8 nM in isolated enzyme assay and 101 nM in human whole blood. PF-8380 has adequate oral bioavailability and exposures required for in vivo testing of autotaxin inhibition. Autotaxin's role in producing LPA in plasma and at the site of inflammation was tested in a rat air pouch model. The specific inhibitor PF-8380, dosed orally at 30 mg/kg, provided >95% reduction in both plasma and air pouch LPA within 3 h, indicating autotaxin is a major source of LPA during inflammation. At 30 mg/kg PF-8380 reduced inflammatory hyperalgesia with the same efficacy as 30 mg/kg naproxen. Inhibition of plasma autotaxin activity correlated with inhibition of autotaxin at the site of inflammation and in ex vivo whole blood. Furthermore, a close pharmacokinetic/pharmacodynamic relationship was observed, which suggests that LPA is rapidly formed and degraded in vivo. PF-8380 can serve as a tool compound for elucidating LPA's role in inflammation.

Autotaxin was first described as a mitogenic factor expressed by a variety of tumor cells, and it causes mitosis and angiogenesis when added to cancer cells (Stracke et al., 1992). It was later determined that autotaxin's mitogenic activity resulted from its lysophospholipase D activity, converting lysophosphatidylcholine (LPC) to lysophosphatidic acid (LPA) (Umezu-Goto et al., 2002). LPA acts through the activation of five G protein-coupled receptors, referred to as LPA1–LPA5 (Ishii et al., 2004), mediating changes in cell survival, proliferation, and migration, tumor cell invasion, lymphocyte infiltration, angiogenesis, and cytokine secretion (Zhao et al., 2008). Both autotaxin and LPA receptors have been found to be up-regulated in many tumor cell lines (Kishi et al., 2006), and LPA induces colony scattering (prerequisite for invasion) in several tumor cells (Shin et al., 2009). Recently, it has been demonstrated that a pan LPA receptor antagonist reduces the size of MDA-MB-231 tumors adapted in rats (Prestwich et al., 2008).

The autotaxin LPA axis has been shown to be up-regulated in a variety of inflammatory conditions. In human rheumatoid arthritis (RA) the autotaxin gene is up-regulated in fibroblasts from patients with RA (Kehlen et al., 2001), and autotaxin protein has been found in the synovial fluid of the patients (Nochi et al., 2008). LPA receptor 1 is up-regulated in synovial fibroblasts from patients with RA (Nochi et al., 2008). Autotaxin is one of four proteins up-regulated in patients with multiple sclerosis as demonstrated by two-dimensional gels (Hammack et al., 2004). LPA1 knockout mice have been shown to be resistant to neuropathic pain produced in a spinal nerve ligation model (Inoue et al., 2004). It has been hypothesized that LPA acts to produce pain by down-regu-

Article, publication date, and citation information can be found at http://jpet.aspetjournals.org.
doi:10.1124/jpet.110.165845.
[S] The online version of this article (available at http://jpet.aspetjournals.org) contains supplemental material.

ABBREVIATIONS: LPA, lysophosphatidic acid; LPC, lysophosphatidylcholine; RA, rheumatoid arthritis; FS-3, fluorescent substrate 3; PF-8380, 6-(3-(piperazin-1-yl)propanoyl)benzo[d]oxazol-2(3*H*)-one; S32826, [4-(tetradecanoylamino)benzyl]phosphonic acid disodium salt; RT, room temperature; DMSO, dimethyl sulfoxide; TEA, triethylamine; DMEM, Dulbecco's modified Eagle's medium; HEK, human embryonic kidney; DMF, dimethylformamide; LC, liquid chromatography; MS/MS, tandem mass spectrometry; PK/PD, pharmacokinetic/pharmacodynamic; AUC, area under the curve.

lating the mammalian K(2P)2.1 (KCNK2, TREK-1) channel (Cohen et al., 2009) and Aβ-fiber-mediated spinal transmission, which underlies neuropathic pain (Xie et al., 2008).

Autotaxin is found in three main isoforms, each with a different splice variant. The most stable and common β isoform is a 95-kDa protein secreted by inflammatory cells and responsible for the production of LPA by the hydrolysis of LPC (produced through secretory phospholipase A2) (Giganti et al., 2008).

Autotaxin has been shown to be responsible for the production of LPA in plasma. Autotaxin heterozygote knockout mice have a 50% reduction of circulating LPA compared with wild-type mice (van Meeteren et al., 2006). Early autotaxin inhibitors have shown that plasma LPA, generated from endogenous LPC by incubating whole blood for several hours, can be nearly 100% inhibited, suggesting that autotaxin is the primary enzyme responsible for LPA production (Ferry et al., 2008). These inhibitors, however, were not suitable for in vivo use because of their limited solubility and bioavailability. One critical question remains: does inhibition of autotaxin reduce LPA levels at the site of inflammation? And if so, what are the consequences of that inhibition?

To date, no autotaxin inhibitors have been developed that regulate LPA levels in vivo; however, there have been several reports of inhibitors that modulate autotaxin in vitro or in whole blood. Inhibitors that have been described are based on substrate analogs (Prestwich et al., 2008). These compounds are weak autotaxin inhibitors and are also LPA1 receptor agonist/antagonists. Recently, S32826 [[4-(tetradecanoylamino) benzyl]phosphonic acid disodium salt] has been described as a potent inhibitor of autotaxin in vitro and in whole blood, but it is not bioavailable or useful for in vivo work (Ferry et al., 2008).

In this article we describe the development of an autotaxin inhibitor that modulates LPA levels in vitro and in vivo through the direct inhibition of autotaxin. The compound is capable of blocking inflammation-induced LPA synthesis, both in plasma and at the site of inflammation. This will allow further testing of the hypothesis that disruption of the autotaxin/LPA axis will have beneficial anti-inflammatory effects that could affect pain and an array of diseases such as RA and cancer.

Materials and Methods

Materials

LPC and LPA were obtained from Avanti Polar Lipids (Birmingham, AL); all standard buffer reagents and solvents were obtained from Sigma-Aldrich (St. Louis, MO).

***tert*-Butyl 4-(3-oxo-3-(2-oxo-2,3-dihydrobenzo[d]oxazol-6-yl) propyl)piperazine-1-carboxylate.** 6-(3-chloropropanoyl)benzo[d] oxazol-2(3*H*)-one (20.0 g, 88.64 mmol) and *tert*-butyl piperazine-1-carboxylate (18.2 g, 97.50 mmol) were dissolved in dichloromethane (200 ml), and triethylamine (37.1 m, 266.0 mmol) was added. The reaction was stirred at room temperature (RT) overnight at which time it was quenched with water (100 ml), and the organics were extracted with dichloromethane (2 × 50 ml). The organics were concentrated and redissolved in a small amount of diethyl ether. The flask was cooled to 0°C, which precipitated pure *tert*-butyl 4-(3-oxo-3-(2-oxo-2,3-dihydrobenzo[d]oxazol-6-yl)propyl)piperazine-1-carboxylate as a white solid (27.18 g, 72.48 mmol, 81%).

6-(3-(Piperazin-1-yl)propanoyl)benzo[d]oxazol-2(3*H*)-one. *tert*-butyl 4-(3-oxo-3-(2-oxo-2,3-dihydrobenzo[d]oxazol-6-yl)propyl)piperazine-1-carboxylate (27.13 g, 72.26 mmol) was dissolved in dioxane (50 ml), and 4 N HCl in dioxane (18.1 ml) was added. The heterogeneous solution was stirred for 1 h at which time the precipitate was filtered to give 6-(3-(piperazin-1-yl)propanoyl)benzo[d]oxazol-2(3*H*)-one as an off-white solid (19.87 g, 100%).

PF-8380. PF-8380 [6-(3-(piperazin-1-yl)propanoyl)benzo[d]oxazol-2(3*H*)-one] (19.87 g, 72.26 mmol) was dissolved in dioxane (50 ml) and water (50 ml) to which sodium bicarbonate (16.1 g, 152 ml) was added. The solution was cooled to 0°C, and 4-nitrochloroformate (19.1 g, 94.4 mmol) was added dropwise. The solution was slowly warmed to RT overnight. The solution was then quenched with water (300 ml), and the resulting precipitate was filtered. In a separate flask (3,5-dichlorophenyl)methanol (13.0 g, 73.20 mmol) was dissolved in DMF (50 ml), and sodium hydride (3.96 g, 99.0 mmol) was added. The solution was stirred for 10 min and cooled to 0°C. The nitro-precipitate was dissolved in DMF (50 ml) and then added dropwise to the (3,5-dichlorophenyl)methanol solution. The solution was stirred for 10 min and then quenched with a small amount of water to ensure quenching of excess sodium hydride. The DMF was distilled off to give a bright yellow oil, which was purified by flash chromatography (5% MeOH/dichloromethane) to give PF-8380 an off-white solid (14.56 g, 30.65 mmol 42%). 1H NMR (400 MHz, DMSO-d6) d ppm 7.83–7.89 (2 H, m), 7.57 (1 H, s), 7.42 (2 H, s), 7.18 (1 H, d, J = 7.9 Hz), 5.07 (2 H, s), 3.37 (3 H, br. s.), 3.19 (2 H, t, J = 7.1 Hz), 2.89 (1 H, s), 2.73 (1 H, s), 2.70 (2 H, t, J = 7.1 Hz), 2.42 (4 H, t, J = 4.7 Hz) C13 NMR (400 MHz, DMSO-d6) 197.35, 154.71, 153.98, 143.37, 141.20, 135.30, 134.03, 130.81, 127.36, 126.08, 124.97, 109.33, 108.77, 64.64, 52.83, 52.25, 43.47, 35.38, *m/z* = 478.1.

Murine Autotaxin Cloning

The full-length murine autotaxin cDNA was purchased from Open Biosystems (Huntsville, AL). The following primers purchased from Integrated DNA Technologies (Coralville, IA) were used to introduce cloning sites HindIII and NotI by polymerase chain reaction to allow cloning into pcDNA3.1 Zeo: 5′-AGC TAG CTA AGC TTA TGG CAA GAC AAG GCT GTT TC-3′ and 5′-ATG ACT GAC TGC GGC CGC TCA TTA GTG ATG ATG GTG GTG ATG AAT CTC GCT CTC ATA TGT ATG CAG G-3′. The 3′ primer introduced the addition of a His6 tag to the C terminus of the protein. The murine autotaxin gene was amplified by using Accuprime Pfx DNA polymerase (Invitrogen, Carlsbad, CA). The DNA sequence of the final construct was confirmed by sequencing performed at Cogenics (Houston, TX).

Autotaxin Expression

Ten-liter batches of human and murine autotaxin-conditioned media were prepared by using a HEK 293 FreeStyle (Invitrogen) and Wave (GE Healthcare, Little Chalfont, Buckinghamshire, UK) bioreactor transient expression system. Approximately 2.5×10^9 HEK cells were seeded into a Wave Bioreactor CellBag20 containing 5 liters of 293 FreeStyle media. The bag was maintained at 37°C, 8% CO_2, and a constant rocking of 25.5 rpm. When the cell density reached 2×10^7/ml, 4.5 liters of fresh 293 FreeStyle media was added. The cells were transfected by the sterile addition of 640 ml of Opti-MEM (Invitrogen) containing 10 mg of plasmid DNA and 13 ml of 293Fectin (Invitrogen). The bioreactor was maintained under the initial growth conditions for another 6 days after transfection, and the media were harvested for purification.

Autotaxin Purification

Concentrated HEK cell media were buffered to pH 8.0 with Trizma preset crystals, and octyl-β-D-pyranoside was added to 0.05% with 300 mM NaCl. Protein was initially captured by using Ni-NTA Superflow resin and further purified by using Q-Sepharose FF resin (QIAGEN, Valencia, CA). Samples containing autotaxin with a purity more than 80% (as determined by SDS-polyacrylamide gel electrophoresis) were pooled, concentrated, and further purified by using a Superdex 200 (16/60) column (GE Healthcare) run in 50 mM Tris (pH 8.0), 150 mM NaCl, and 0.05% octyl-β-D-pyranoside. Fractions

containing autotaxin with purity more than 95% were pooled, concentrated, and stored at −80°C.

Recombinant Enzyme Assay

FS-3 substrate (Echelon L-2000; Echelon Biosciences, Logan, UT) was solubilized in assay buffer at 500 μM and frozen at −20°C in single-use aliquots for up to 4 weeks. Recombinant autotaxin was diluted in Tris-buffered saline (140 mM NaCl, 5 mM KCl, 1 mM $CaCl_2$, 1 mM $MgCl_2$, 50 mM Tris, pH 8.0) and incubated with compound in DMSO or DMSO alone (final 1% DMSO) for 15 min at 37°C, and the reaction was started with the addition of FS-3 at a final concentration of 1 μM. The reaction was allowed to proceed at 37°C for 30 min and monitored at 520 nm until the uninhibited control compared with a no-enzyme control gave a $Z' \geq 0.5$. IC_{50}s were determined in triplicate by using a four-parameter fit.

Recombinant Enzyme Assay Using LPC LC-MS/MS

C17:0 LPC and C16:0 LPA were dissolved in MeOH (10 and 100 mg/ml, respectively) and maintained at −20°C. Recombinant autotaxin was diluted in Dulbecco's modified Eagle's medium (DMEM) and added to compound in DMSO or DMSO alone (final 1% DMSO), and the reaction was started with the addition of LPC at a final concentration of 15 μl/ml followed by incubation at 37°C for 30 min. The reaction was stopped by the addition of two volumes of organic (50:50:1 acetonitrile/methanol/acetic acid + 15 ng/ml C16:0 LPA, internal standard) and either frozen at −80°C or diluted further in preparation for LC-MS/MS. Autotaxin LPC assay was diluted 3:7 with 66% methanol/water plus 0.1% triethylamine (TEA) and analyzed by LC-MS/MS.

Fetal Fibroblast Cell Assay

Human fetal fibroblasts were prepared from foreskin and cultured as described previously (Hawley-Nelson et al., 1980; Raz et al., 1989). Cells were grown in DMEM containing 10% fetal bovine serum, 4 mM L-glutamine, 25 mM HEPES, 100 U/ml penicillin, and 100 μg/ml streptomycin (Invitrogen) and were passed when confluent. The cells were suspended in fetal bovine serum-free DMEM and plated at density of 5×10^4 cells/well on 96-well culture plates (Corning Glassworks, Corning, NY). After 24 h of incubation, various concentrations of compound were added with tyrosine protein phosphatase inhibitor cocktail (Millipore Bioscience Research Reagents, Temecula, CA). After 15-min incubation, the substrate C17:0 LPC (final 15 μg/ml) was added to start the autotaxin enzyme reaction. After 30 min at 37°C, the supernatant of cell culture was collected and mixed with organic solution, acetonitrile/methanol/acetic acid (50:50:1, v/v/v) (EMD Chemicals, Gibbstown, NJ), to stop the reaction. C17:0 LPA content was measured by LC-MS/MS.

Autotaxin Inhibition in Human Whole Blood

Venous blood from healthy human donors was collected in heparinized tubes. Blood (0.5 ml) was incubated with compound dissolved in DMSO (1% final concentration of DMSO) in 96-well collection plates for 2 h at 37°C. The reaction was stopped by centrifugation at 800*g* for 10 min to pellet the cells. Plasma supernatant (100 μl) was precipitated with three volumes of methanol/acetonitrile/acetic acid (60:40:1) and spun at 4,000*g* for 10 min. Supernatants were recovered and diluted. LPA was measured by LC-MS/MS. Ten concentrations of compound starting at 10 μM with 3-fold dilutions were examined in duplicate. IC_{50} values were generated by fitting the data with a four-parameter logistic regression fit then determining the point that intersects 50% of the difference between negative (time 0) and positive (2 h) uninhibited controls (control IC_{50}).

LPA Mass Spectrometry

Panels of LPA species including C16:0, C18:0, C18:1, and C20:4 were analyzed by using an LC-MS/MS method modified from the published method by Chen et al. (2008). In brief, 50 μl of sample was extracted with 350 μl of acetonitrile/methanol/acetic acid (50:50:1) containing C17:0 LPA at 5 ng/ml as internal standard. Then, 300 μl of supernatant was removed and 700 μl of methanol/water/TEA (66:34:0.1) was added before analysis. Quantitation experiments were performed by two-dimensional LC-MS/MS by using an HP 1200 LC system (Agilent Technologies, Santa Clara, CA) composed of a quaternary pump, a CTC Analytics HTS PAL autosampler (LEAP Technologies, Carrboro, NC), and a switching valve, plumbed in-line with a HP 1100 high-performance liquid chromatography pump that was interfaced to an API 4000 Qtrap mass spectrometer (MDS-Sciex, Toronto, Canada) operated in the negative ion electrospray and multiple-reaction monitoring modes. Typically, 300 μl of sample was injected onto a Betasil C18 column (Thermo Fisher Scientific, Waltham, MA) with 1 ml/min of 25 mM ammonium acetate/methanol (50:50) mixture. After 3 min, the valve was switched, and the captured analytes were eluted onto a 3.0 × 50-mm, 3.5-μm (particle size) XBridge C8 analytical column (Waters, Milford, MA) with a 3-min gradient at a flow rate of 0.8 ml/min. Gradient mobile phases were methanol/methylene chloride/water (55:5:40) with 0.1% TEA and methanol/methylene chloride (50:50) with 0.1% TEA.

Selected analytes were specifically detected by monitoring high-performance liquid chromatography retention times and ion pairs corresponding to the parent and specific fragment ion mass-to-charge ratios.

Rat Pharmacokinetics

Male Lewis rats weighing 275 to 300 g were purchased from Charles River Laboratories, Inc. (Wilmington, MA) and acclimated to their surroundings for approximately 1 week with food and water provided ad libitum. A minimum of 1 day before study, animals were anesthetized with isoflurane (to effect) and implanted with Culex (BASi, West Lafayette, IN) vascular catheters in the carotid artery. Animals were acclimated in Culex cages overnight before dosing. Patency of the carotid artery catheter was maintained by using the "tend" function of the Culex automated blood sampler. Animals were dosed with PF-8380 at 1, 3, 10, 30, and 100 mg/kg by oral gavage after an overnight fast. Blood collections were obtained from the carotid artery and performed by the Culex automated blood sampler at 0.25, 0.5, 1, 2, 4, 6, 8, and 24 h after administration. Blood was centrifuged, and plasma was collected for analysis of PF-8380 and LPA concentrations.

Pharmacodynamic Modeling

The LPA data obtained during the rat pharmacokinetic study were fit to the inhibitory E_{max} pharmacodynamic model described by the following equation:

$$E = E_{max} - (E_{max} - E_0) \times \left(\frac{C_p}{C_p + EC_{50}}\right) \quad (1)$$

where the effect (E) is E_{max} at a plasma concentration of zero ($C_p = 0$) and E_0 as the plasma concentration approaches infinity ($C_p = \infty$). EC_{50} represents the concentration required to achieve 50% of the maximal inhibitory effect. Pharmacodynamic modeling was conducted by using all plasma concentration and LPA concentration data with WinNonlin version 5.2 (Pharsight, Mountain View, CA).

Sample Preparation and LC-MS/MS Analysis of Plasma for PF-8380

Fifty microliters of plasma was mixed with 150 μl of acetonitrile containing LPA 17:0 internal standard and centrifuged to pellet-precipitated proteins. Supernatant from each sample was analyzed on a Sciex API4000 LC-MS/MS system equipped with two Shimadzu (Kyoto, Japan) LC-10AD VP binary pumps and LEAP HTC PAL autosampler. A 5-μl sample extract was injected onto a Thermo Fisher Scientific Aquasil C18 (2.1 × 30 mm, 3 μm) analytical column and eluted by using a linear gradient with mobile phase consisting of 0.1% formic acid and 0.1% formic acid in acetonitrile. PF-8380 was

analyzed by using Turbo IonSpray (MDS-Sciex) in ESI+ mode with multiple-reaction monitoring of parent/daughter ions at *m/z* 478.1/161.0.

Carrageenan-Induced LPA in the Rat Air Pouch

Male Lewis rats (175–200 g; Charles River Laboratories) were used in the study. Air pouches were produced by subcutaneous injection of 20 ml of sterile air into the intrascapular area of the back. Pouches were allowed to develop for 1 day. Animals (six per group) were fasted with free access to water for 16 to 24 h before drug administration. Drug, vehicle, or 1 mg/kg dexamethazone were administered by oral gavage 1 h before injection of 2 ml of a 1% suspension of carrageenan (FMC BioPolyer, Philadelphia PA) dissolved in saline into the pouch. At 3 h after carrageenan injection, the pouch fluid was collected by lavage with 2 ml of phosphate-buffered saline containing 10 μM sodium fluoride (Sigma-Aldrich). The fluid was centrifuged at 800*g* for 10 min at 4°C, and the supernatants were collected for LPA analysis by LC-MS/MS. Blood samples were collected into 10-ml heparinized tubes (Vacutainer tubes; BD Biosciences, Franklin Lakes NJ) 4 h after dosing and immediately centrifuged at 800*g* for 10 min at 4°C and then frozen at −80°C. For analysis of autotoxin activity, samples of both pouch and plasma were incubated at room temperature for 4 h. LPA was produced from existing LPC and autotoxin levels in those fluids. The difference in LPA levels from time 0 to 4 h was used to calculate autotoxin activity.

Rat Adjuvant-Induced Arthritis Hyperalgesia

Inflammation was established in female Lewis rats (150–200 g; Harlan, Indianapolis, IN). Five animals per dose group were injected with 3 mg/kg heat-killed *Mycobacterium butyricum* suspended in paraffin oil subcutaneously on the base of the tail (day 0). By days 10 to 14 rats manifested signs of disease, and vocalization baselines were taken by flexing the right and left knees 10 times each. Rats that vocalized at least five times/hind legs were included in the study. Animals were treated orally b.i.d. with 10, 30, or 100 mg/kg PF-8380, 30 mg/kg naproxen (positive control), or vehicle, and vocalization was assessed on day 3, 2 h after administration.

Animal Use

The Pfizer Institutional Animal Care and Use Committee reviewed and approved the animal use in these studies. The animal care and use program is fully accredited by the Association for Assessment and Accreditation of Laboratory Animal Care International.

Results

PF-8380. Screening of our compound collection identified numerous leads for our medicinal chemistry program. Our medicinal chemistry effort rapidly optimized the lead matter by improving potency and pharmacokinetics properties, resulting in the identification of PF-8380 (Fig. 1) as a suitable tool compound for in vivo evaluation.

In Vitro Potency. Potency of PF-8380 was confirmed as low nanomolar by using several assay methods. Each method differed by substrate and sources/species of enzyme. The data are summarized in Table 1. Recombinant human enzyme (β isoform) purified from HEK293 cells was used with the high-throughput screening assay of the fluorescent substrate FS-3 and LPC 17:0 as substrates. Both substrates were run at similar enzyme concentrations (approximately 5 nM) and incubation and reaction times. Both substrates gave similar low-nanomolar IC_{50}s. PF-8380 also inhibited rat autotaxin with an IC_{50} of 1.16 nM with FS-3 substrate. Potency of PF-8380 was maintained when using enzyme produced from fetal fibroblasts used in combination with LPC as a substrate. In human whole blood incubated with compound for 2 h autotaxin was inhibited with an IC_{50} of 101 nM.

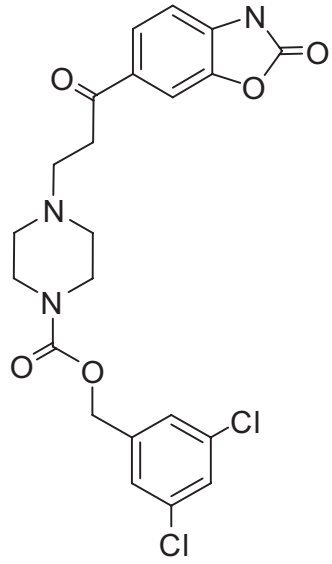

Fig. 1. Structure of PF-8380.

TABLE 1
In vitro potency of PF-8380

Assay	IC_{50}
	nM ± *S.D.*
Human enzyme FS-3	2.8 ± 0.16 (n = 4)
Human enzyme LPC	1.7 ± 0.6 (n = 3)
Murine enzyme FS-3	1.16 ± 0.07 (n = 3)
Fetal fibroblast cell LPC	1.15 ± 0.18 (n = 3)
Human whole blood	101 ± 0.036 (n = 3)

Pharmacokinetics. The pharmacokinetic profile of PF-8380 was evaluated at an intravenous dose of 1 mg/kg and oral doses of 1 to 100 mg/kg out to 24 h (Fig. 2, A and B). PF-8380 had mean clearance of 31 ml/min/kg, volume of distribution at steady state of 3.2 l/kg, and effective $t_{1/2}$ of 1.2 h (Table 2). Oral bioavailability was moderate, ranging from 43 to 83% (Table 2). Plasma concentrations increased with single oral escalating doses (Fig. 2B), but C_{max} increased at a rate that was approximately proportional to dose from 1 to 10 mg/kg and less than proportional to dose from 10 to 100 mg/kg (Fig. 2C). PF-8380 exposures estimated by area under the curve were approximately proportional to dose and linear up to 100 mg/kg (Fig. 2C). Plasma C16:0, C18:0, and C20:0 LPA levels were measured immediately after collection (Fig. 2D shows C18:0 LPA levels at all doses). Maximal reduction of LPA levels was observed by the 3 mg/kg dose at 0.5 h with all LPA returning at or above baseline at 24 h.

PF-8380 Pharmacodynamics. The pharmacodynamic effect of PF-8380 was measured as decreasing C16:0, C18:0, and C20:0 LPA levels in the plasma. The plasma LPA levels and PF-8380 concentrations were fit to an inhibitory E_{max} model, and the model parameters (EC_{50}, E_{max}, and E_0) for each LPA are presented in Table 3. The effect of PF-8380 on plasma LPA levels indicated a direct response (Supplemental Figs. 1–4). Data show that LPA concentrations declined rapidly and reached their maximal inhibition between 15 and 30 min after administration for all doses levels, corresponding with PF-8380 plasma t_{max} (Table 2). It is interesting to note

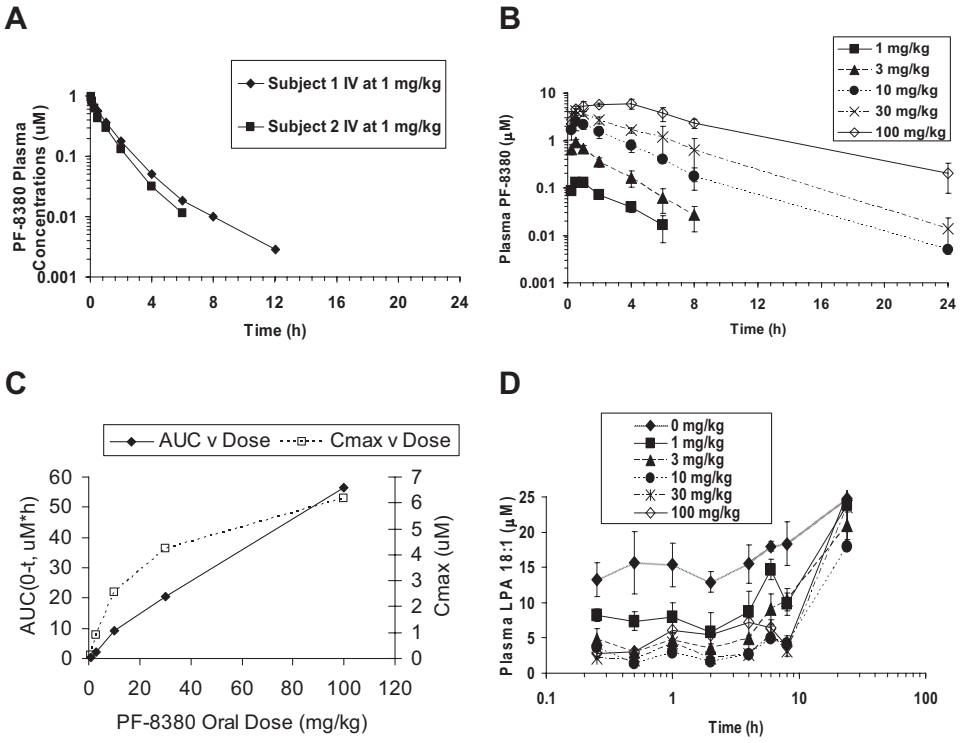

Fig. 2. Pharmacokinetics of PF-8380 in rat. A, plasma concentration-time profile after intravenous administration of 1 mg/kg PF-8380 to Wistar rats. B, plasma concentration-time profile after various single oral doses. C, exposures at C_{max} and AUC by dose. D, plasma concentration-time profiles of LPA 18:1 levels ± S.E.M. immediately after collection.

TABLE 2
Pharmacokinetics of PF-8380 in rat

Parameter	Units	Intravenous 1 mg/kg (n = 2)	Oral 1 mg/kg (n = 5)	Oral 3 mg/kg (n = 3)	Oral 10 mg/kg (n = 3)	Oral 30 mg/kg (n = 3)	Oral 100 mg/kg (n = 3)
Dose	mg/kg	1	1	3	10	30	100
AUC	μM·h	1.12	0.480 ± 0.120	2.25 ± 0.54	9.22 ± 2.75	20.6 ± 6.2	56.6 ± 11.0
Clearance	ml/min/kg	31					
V_{dss}	l/kg	3.2					
C_{max}	μM		0.124 ± 0.025	0.922 ± 0.120	2.55 ± 0.75	4.23 ± 0.50	6.19 ± 1.06
T_{max}	h		0.60 ± 0.22	0.50 ± 0.0	0.67 ± 0.29	0.42 ± 0.14	3.3 ± 1.2
Effective $t_{1/2}$	h	1.2					
Terminal $t_{1/2}$	h	1.7	2.1 ± 0.7	1.5 ± 0.2	2.2 ± 0.5	2.8 ± 0.3	4.3 ± 1.2
Bioavailability	%		43 ± 9	68 ± 16	83 ± 25	62 ± 19	52 ± 10

TABLE 3
Inhibitory E_{max} model parameters

	C16:0 (95% CI)	C18:0 (95% CI)	C20:0 (95% CI)
EC_{50} (nmol/l)	54.7 (31.1–78.3)	84.6 (19.7–149)	51.7 (29.1–74.3)
E_{max} (ng/ml)	19.6 (18.4–20.8)	15.9 (14.2–17.6)	276.7 (259.4–293.9)
E_0 (ng/ml)	3.25 (2.30–4.21)	3.10 (1.64–4.56)	48.3 (34.8–61.7)

that the EC_{50} values obtained (means = 51.7–84.6 nM) were similar to the IC_{50} value obtained from human whole blood in the in vitro potency assay (Table 1).

In Vivo Modulation of LPA Levels. Reduction of LPA in vivo, both in plasma and at the site of inflammation, was evaluated in a rat air pouch model of inflammation. PF-8380 was dosed orally and provided dose-proportional blood levels from 0.079 μM at 3 mg/kg to 2.68 μM at 100 mg/kg at 4 h after dose. LPA was evaluated from plasma and pouch fluid immediately after collection and after a 4-h incubation (Fig. 3). Autotaxin activity was calculated as a formation rate of LPA (Fig. 4). Autotaxin was inhibited up to 95% in both plasma and air pouch at 100 mg/kg. Dose-responsive inhibition of autotaxin activity in plasma and pouch was correlated with human whole blood (Fig. 5). EC_{60} was approximately 0.08 μM for inhibition in human whole blood, in vivo rat plasma, and rat air pouch, and EC_{90} was approximately 2 μM for all three (human whole blood, plasma, and pouch).

Inhibition of Inflammatory Hyperalgesia. Using vocalization as a measure of inflammatory hyperalgesia, PF-8380 reduced hyperalgesia in a dose-responsive manner with the same efficacy as 30 mg/kg naproxen (Fig. 6). PF-8380 had maximal efficacy at 30 mg/kg compared with 30 mg/kg naproxen. This dose corresponded to maximal inhibition of LPA levels both in plasma and the site of inflammation.

Discussion

A high-throughput screening assay for autotaxin inhibitors using FS-3 produced many potent chemical series. A handful of inhibitors of autotaxin have appeared in the literature (Parrill and Baker 2008). A recent report claimed a series of autotaxin inhibitors, inspiring us to engage in a structure–activity relationship aimed at identifying a suitable tool compound (Schiemann et al., 2009). Our medicinal chemistry effort rapidly explored the structure–activity relationship in this lead series with a focus on improved potency and pharmacokinetics properties, resulting in the identification of PF-8380 as a suitable tool compound for in vivo evaluation.

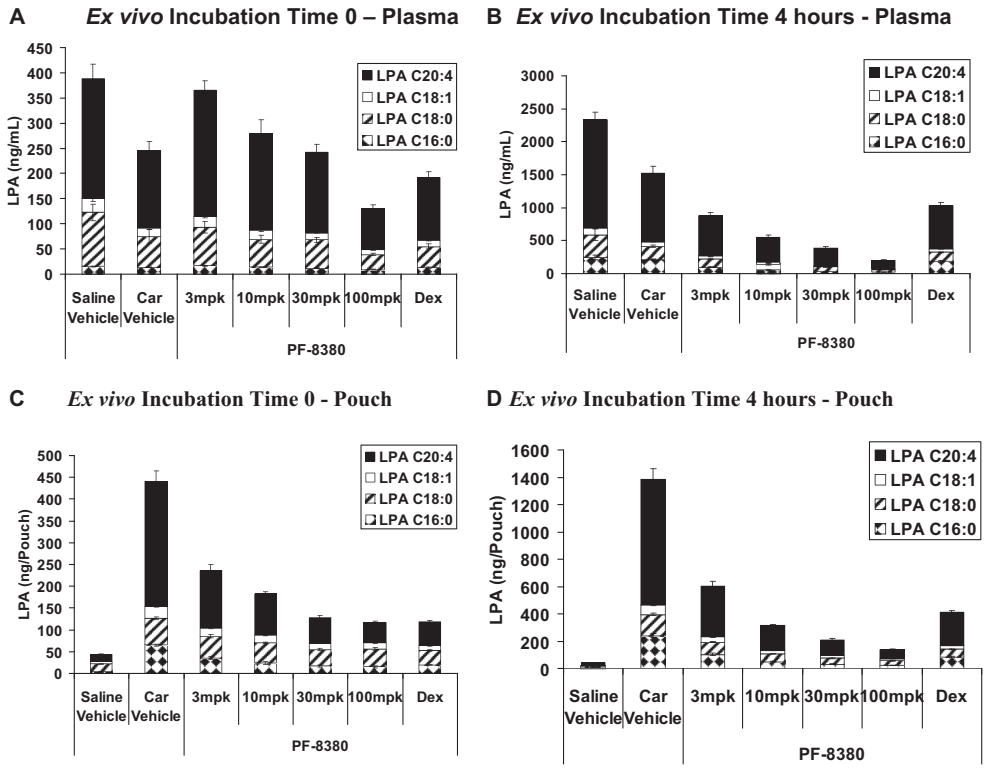

Fig. 3. In vivo inhibition of LPA generation by PF-8380. Various amounts of PF-8380 or dexamethasone (Dex) (1 mg/kg) were dosed orally 1 h before injection of carrageenan in rat air pouch (n = six rats per group). Three hours after carrageenan injection plasma and pouch fluid were collected, and LPA was analyzed by mass spectrometry. Plotted are total LPA of four major species immediately after collection from plasma (A) and air pouch (B) and 4-h incubation at RT for plasma (C) and air pouch (D).

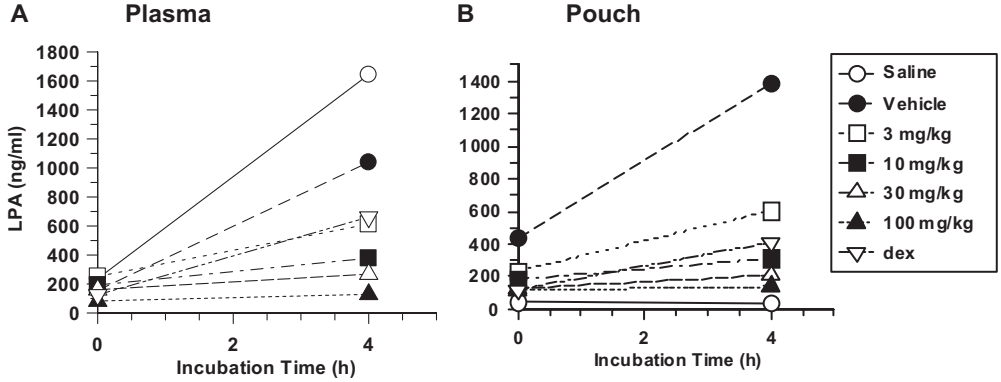

Fig. 4. In vivo inhibition of autotaxin activity by PF-8380. Autotaxin activity inhibition was measured by incubation of rat plasma (A) and pouch fluid (B) for 4 h at RT. Plotted is the average total LPA measured by mass spectrometry from six animals per group. dex, dexamethasone.

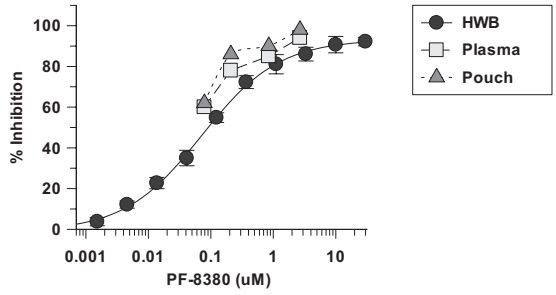

Fig. 5. Correlation of autotaxin activity inhibition in human whole blood (HWB), rat plasma, and rat air pouch. Percentage of inhibition of autotaxin activity is plotted versus concentration of PF-8380 for human whole blood, rat plasma, and rat inflammatory air pouch 4 h after oral dosing and 3 h after carrageenan. Autotaxin activity was determined as the rate of formation of LPA 18:1 for 4 h at RT. Human whole blood is the average ± S.E.M. for three donors. In vivo plasma and pouch is the percentage of inhibition of an average of six animals per group.

When these were tested further using LPC either as a substrate or enzyme produced from a cell line, many series were much less potent. The series, which included PF-8380, maintained their potency both when using LPC or FS-3 as a substrate and either recombinant or enzyme secreted by fetal fibroblast cells. Subsequent analogs synthesized within this series produced PF-8380, with nanomolar potency in enzyme assays and 100 nM potency in human whole blood. Several observations suggest that PF-8380 is a tight-binding inhibitor of autotaxin with subnanomolar potency. PF-8380 seems to be competitive with substrate (data not shown). Traditional kinetic analysis was complicated by apparent substrate inhibition in the FS-3 substrate assay with a K_m of approximately 3 μM and a K_i for substrate inhibition of the enzyme-substrate complex of approximately 13 μM. However, IC_{50}s of PF-8380 determined at 1, 5, 10, and 20 μM substrate showed little effect of substrate escalation on the IC_{50}. Rather than the 6-fold increase in IC_{50} between 1 and 20 μM expected for a competitive inhibitor, an increase of only 1.2-fold was observed. This suggests that the K_i for PF-8380 is much smaller than the enzyme concentration in the assay (2–5 nM). In fact, the slope and intercept of a plot of IC_{50} versus substrate concentration were consistent with a

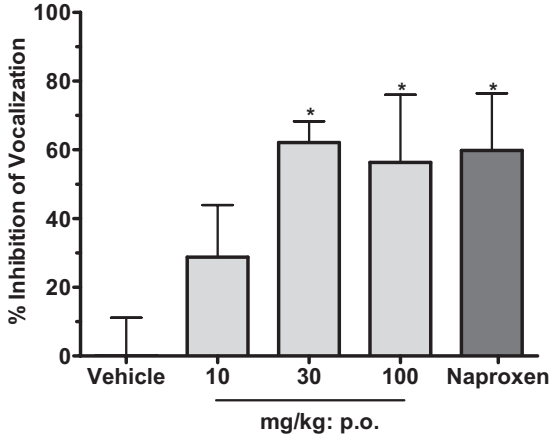

Fig. 6. Inhibition of hyperalgesia associated with adjuvant-induced arthritis by PF-8380. Female Lewis rats (five animals per dose group) were treated orally b.i.d. with 10, 30, or 100 mg/kg PF-8380 or 30 mg/kg naproxen (positive control), and vehicle and vocalization were assessed on day 3, 2 h after administration. Plotted is the average percentage of inhibition of vehicle versus control ± S.E.M.

K_i of approximately 0.04 nM and an enzyme concentration of 2.2 nM (data not shown). In addition, a direct fit of enzyme activity versus inhibitor concentration data using the Morrison equation for tight-binding inhibitors yielded a K_i of 0.02 nM and an enzyme concentration of 2.6 nM (data not shown). These observations indicate that under the conditions of the recombinant enzyme assays PF-8380 is essentially titrating the enzyme active site.

Because most preclinical animal models are done in rodents, the potency of PF-8380 was evaluated against rat autotaxin. Rat and murine autotaxin sequences are identical, so these measurements can be used for either species. The potency in the recombinant enzyme assay was comparable with human. A determination was made that human whole-blood assays could be used to estimate potency in a rodent system. Human whole-blood potency was shifted as expected to the right, probably because of protein binding. PF-8380 inhibited plasma autotaxin activity >90%, indicating that it is the major source of LPA production in plasma.

Analysis of a pharmacokinetic/pharmacodynamic (PK/PD) relationship was attempted by measuring plasma LPA. Our initial observations with human whole blood and the observation in autotaxin heterozygote knockout animals indicate that autotaxin is the major source of LPA in plasma. To determine a PK/PD effect, however, the rate of biosynthesis/degradation of LPA needs to be taken into account. Whole-blood assays depend on an incubation period from several hours up to 24 h to produce LPA from plasma autotaxin activity. Our analysis was careful to limit the time of incubation of the plasma after sampling, but with many time points it was difficult to obtain samples at precisely the right time, meaning that there was most certainly some incubation time. In any event, LPA levels were rapidly reduced after oral dosing, indicating that LPA present at basal levels in the plasma is rapidly degraded.

Analysis of the in vivo effects of PF-8380 on production of LPA in plasma and the inflamed air pouch indicates a close correlation between plasma, pouch, and ex vivo whole-blood inhibition of autotaxin activity. Plasma and pouch samples were collected immediately and processed for LPA analysis. Plasma samples without incubation to determine autotaxin activity did not show a dose-dependent decrease in LPA as was seen in the PK study. Plasma that was incubated for 4 h at RT showed a very good dose response. This indicated that basal LPA levels are not as sensitive to autotaxin inhibition and that analysis of autotaxin activity needs to be performed to determine a PK/PD relationship. Pouch samples, on the other hand, either with 4 h of incubation or no incubation, showed a similar dose response. Presumably the pouch, with a robust inflammatory condition, produces much more autotaxin, hence higher basal levels of LPA, and it is sensitive to autotaxin inhibition.

To estimate doses necessary to inhibit LPA formation in vivo at the site of inflammation, a correlation of human whole-blood inhibition of plasma autotaxin activity and air pouch autotaxin activity indicate that there is a close correlation of the three. This suggests that a whole-blood assay can be an accurate measure of subsequent doses needed to completely inhibit the production of LPA at the site of inflammation. Autotaxin's role in the production of LPA at the site of inflammation was then tested with PF-8380. Immediately after samples were taken from the pouch LPA levels were analyzed, which minimized LPA formation by autotaxin activity in the fluid. LPA levels in the pouch were inhibited >90%, indicating that autotaxin is the primary source of LPA at the site of inflammation. PF-8380 was evaluated for its inhibition of inflammatory hyperalgesia in rat adjuvant-induced arthritis. Maximal efficacy in hyperalgesia was equal to naproxen at 30 mg/kg. In previous studies, naproxen dosed orally at 10 mg/kg was determined from biomarker data to be efficacious to inhibit PGE2 and thus both forms of cyclooxygenase. A dose of naproxen three times higher was used in this study, which represents maximal effect based on cyclooxygenase. Naproxen at 100 mg/kg produces side effects in rats, such as a gastrointestinal side effect, that will not provide mechanism-based data; therefore, we did not test doses higher than 30 mg/kg. This indicated that hyperalgesia caused by adjuvant-induced arthritis is primarily peripheral, because the LPA biomarkers in this study were peripheral measures of LPA reduction.

In summary, this is the first report of an inhibitor of autotaxin that reduces LPA levels in vivo. PF-8380 has been demonstrated to be a potent inhibitor of autotaxin in vitro by using native enzyme and substrate and also in ex vivo human whole blood. PF-8380 is bioavailable and can be dosed in vivo to levels that are several multiples above the ED_{80}, which can be accomplished with twice a day dosing at 10 mg/kg. Autotaxin's role in the production of LPA at the site of inflammation was confirmed in the rat air pouch model of inflammation. Autotaxin was inhibited >90% both in plasma and at the site of inflammation by PF-8380, indicating that autotaxin is the primary enzyme responsible for the production of LPA at the site of inflammation. Measurement of autotaxin activity in ex vivo whole blood or plasma can be used to calculate dose projections, and PF-8380 can now be used as a pharmacological tool to evaluate the role that LPA plays in inflammation and cancer.

Acknowledgments

We thank Pat Griffin of The Scripps Institute (Jupiter, Florida) for the human autotaxin clone and initial high-throughput assay development and James Valentine, Karen Mattison, Mark Tibbetts, and

Steve Hawrylik of the Pfizer Biomolecular Screening Group for screening the Pfizer compound library for initial autotaxin hits.

References

Chen YQ, Kuo MS, Li S, Bui HH, Peake DA, Sanders PE, Thibodeaux SJ, Chu S, Qian YW, Zhao Y, et al. (2008) AGPAT6 is a novel microsomal glycerol-3-phosphate acyltransferase. *J Biol Chem* **283:**10048–10057.

Cohen A, Sagron R, Somech E, Segal-Hayoun Y, and Zilberberg N (2009) Pain-associated signals, acidosis and lysophosphatidic acid, modulate the neuronal K(2P)2.1 channel. *Mol Cell Neurosci* **40:**382–389.

Ferry G, Moulharat N, Pradère JP, Desos P, Try A, Genton A, Giganti A, Beucher-Gaudin M, Lonchampt M, Bertrand M, et al. (2008) S32826, a nanomolar inhibitor of autotaxin: discovery, synthesis and applications as a pharmacological tool. *J Pharmacol Exp Ther* **327:**809–819.

Giganti A, Rodriguez M, Fould B, Moulharat N, Cogé F, Chomarat P, Galizzi JP, Valet P, Saulnier-Blache JS, Boutin JA, et al. (2008) Murine and human autotaxin α, β, and γ isoforms: gene organization, tissue distribution, and biochemical characterization. *J Biol Chem* **283:**7776–7789.

Hammack BN, Fung KY, Hunsucker SW, Duncan MW, Burgoon MP, Owens GP, and Gilden DH (2004) Proteomic analysis of multiple sclerosis cerebrospinal fluid. *Mult Scler* **10:**245–260.

Hawley-Nelson P, Sullivan JE, Kung M, Hennings H, and Yuspa SH (1980) Optimized conditions for the growth of human epidermal cells in culture. *J Invest Dermatol* **75:**176–182.

Inoue M, Rashid MH, Fujita R, Contos JJ, Chun J, and Ueda H (2004) Initiation of neuropathic pain requires lysophosphatidic acid receptor signaling. *Nat Med* **10:**712–718.

Ishii I, Fukushima N, Ye X, and Chun J (2004) Lysophospholipid receptors: signaling and biology. *Annu Rev Biochem* **73:**321–354.

Kehlen A, Lauterbach R, Santos AN, Thiele K, Kabisch U, Weber E, Riemann D, and Langner J (2001) IL-1β- and IL-4-induced down-regulation of autotaxin mRNA and PC-1 in fibroblast-like synoviocytes of patients with rheumatoid arthritis (RA). *Clin Exp Immunol* **123:**147–154.

Kishi Y, Okudaira S, Tanaka M, Hama K, Shida D, Kitayama J, Yamori T, Aoki J, Fujimaki T, and Arai H (2006) Autotaxin is overexpressed in glioblastoma multiforme and contributes to cell motility of glioblastoma by converting lysophosphatidylcholine to lysophosphatidic acid. *J Biol Chem* **281:**17492–17500.

Nochi H, Tomura H, Tobo M, Tanaka N, Sato K, Shinozaki T, Kobayashi T, Takagishi K, Ohta H, Okajima F, et al. (2008) Stimulatory role of lysophosphatidic acid in cyclooxygenase-2 induction by synovial fluid of patients with rheumatoid arthritis in fibroblast-like synovial cells. *J Immunol* **181:**5111–5119.

Parrill AL and Baker DL (2008) Autotaxin inhibition: challenges and progress toward novel anti-cancer agents. *Anticancer Agents Med Chem* **8:**917–923.

Prestwich GD, Gajewiak J, Zhang H, Xu X, Yang G, and Serban M (2008) Phosphatase-resistant analogues of lysophosphatidic acid: agonists promote healing, antagonists and autotaxin inhibitors treat cancer. *Biochim Biophys Acta* **1781:**588–594.

Raz A, Wyche A, and Needleman P (1989) Temporal and pharmacological division of fibroblast cyclooxygenase expression into transcriptional and translational phases. *Proc Natl Acad Sci USA* **86:**1657–1661.

Schiemann K, Schultz M, Blaukat A, and Kober I (2009), inventors; Merck, assignee. Preparation of piperidines and piperazines as antitumor agents. World patent application WO2009046841. 2009 April 16.

Shin KJ, Kim YL, Lee S, Kim DK, Ahn C, Chung J, Seong JY, and Hwang JI (2009) Lysophosphatidic acid signaling through LPA receptor subtype 1 induces colony scattering of gastrointestinal cancer cells. *J Cancer Res Clin Oncol* **135:**45–52.

Umezu-Goto M, Kishi Y, Taira A, Hama K, Dohmae N, Takio K, Yamori T, Mills GB, Inoue K, Aoki J, et al. (2002) Autotaxin has lysophospholipase D activity leading to tumor cell growth and motility by lysophosphatidic acid production. *J Cell Biol* **158:**227–233.

van Meeteren LA, Ruurs P, Stortelers C, Bouwman P, van Rooijen MA, Pradère JP, Pettit TR, Wakelam MJ, Saulnier-Blache JS, Mummery CL, et al. (2006) Autotaxin, a secreted lysophospholipase D, is essential for blood vessel formation during development. *Mol Cell Biol* **26:**5015–5022.

Xie W, Matsumoto M, Chun J, and Ueda H (2008) Involvement of LPA1 receptor signaling in the reorganization of spinal input through Aβ-fibers in mice with partial sciatic nerve injury. *Mol Pain* 15:46.

Zhao C, Fernandes MJ, Prestwich GD, Turgeon M, Di Battista J, Clair T, Poubelle PE, and Bourgoin SG (2008) Regulation of lysophosphatidic acid receptor expression and function in human synoviocytes: implications for rheumatoid arthritis? *Mol Pharmacol* **73:**587–600.

Address correspondence to: James Gierse, Pfizer Inflammation Research, 700 Chesterfield Parkway N., Chesterfield, MO 63017. E-mail: gierse@sbcglobal.net

A Novel Autotaxin Inhibitor Reduces Lysophosphatidic Acid Levels in Plasma and the Site of Inflammation

James Gierse*, Atli Thorarensen, Konstantine Beltey, Erica Bradshaw-Pierce, Luz Cortes-Burgos, Troii Hall, Amy Johnston, Michael Murphy, Olga Nemirovskiy, Shinji Ogawa, Lyle Pegg, Matthew Pelc, Michael Prinsen, Mark Schnute, Jay Wendling, Steve Wene, Robin Weinberg, Arthur Wittwer, Ben Zweifel and Jaime Masferrer

Figure S1. Plasma PF-8380 and LPA concentrations following a 30 mg/kg oral dose in rats. PF-8380 concentrations are represented by black closed symbols and solid lines and LPA concentrations are represented by gray open symbols and dashed lines. PF-8380 and LPA concentrations are plotted as a function of time.

A.

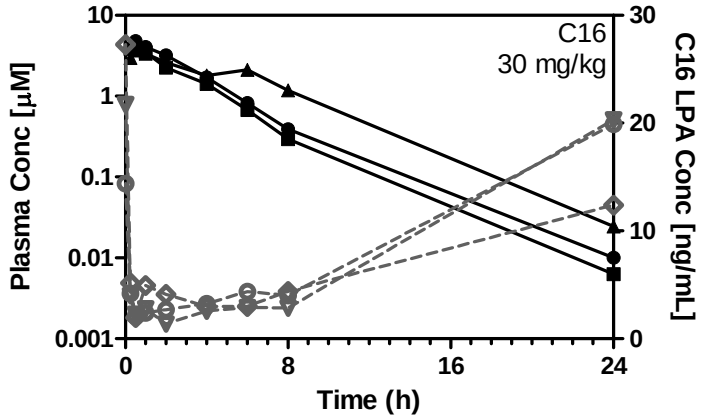

B.

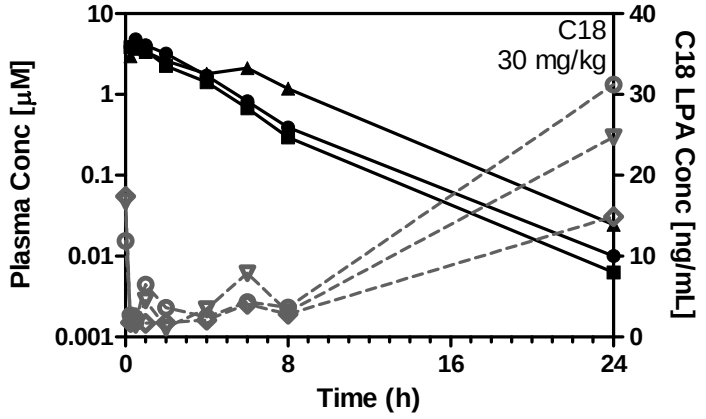

C.

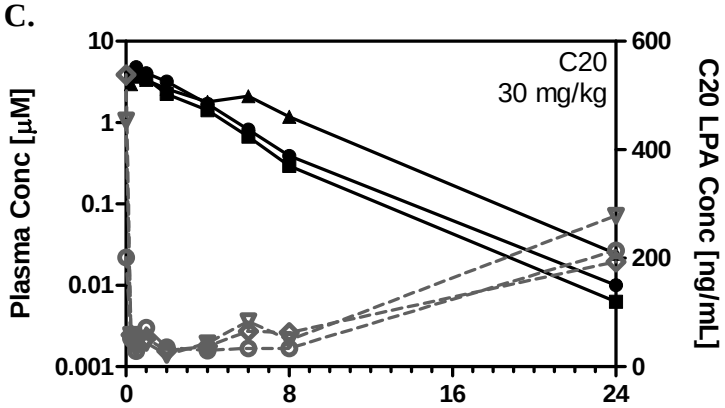

A Novel Autotaxin Inhibitor Reduces Lysophosphatidic Acid Levels in Plasma and the Site of Inflammation

James Gierse*, Atli Thorarensen, Konstantine Beltey, Erica Bradshaw-Pierce, Luz Cortes-Burgos, Troii Hall, Amy Johnston, Michael Murphy, Olga Nemirovskiy, Shinji Ogawa, Lyle Pegg, Matthew Pelc, Michael Prinsen, Mark Schnute, Jay Wendling, Steve Wene, Robin Weinberg, Arthur Wittwer, Ben Zweifel and Jaime Masferrer

Figure S2. C16:0 LPA concentrations as a function of plasma PF-8380 concentration for doses ranging from 0-100 mg/kg. Data points on the graphs are the corresponding blood collection time points.

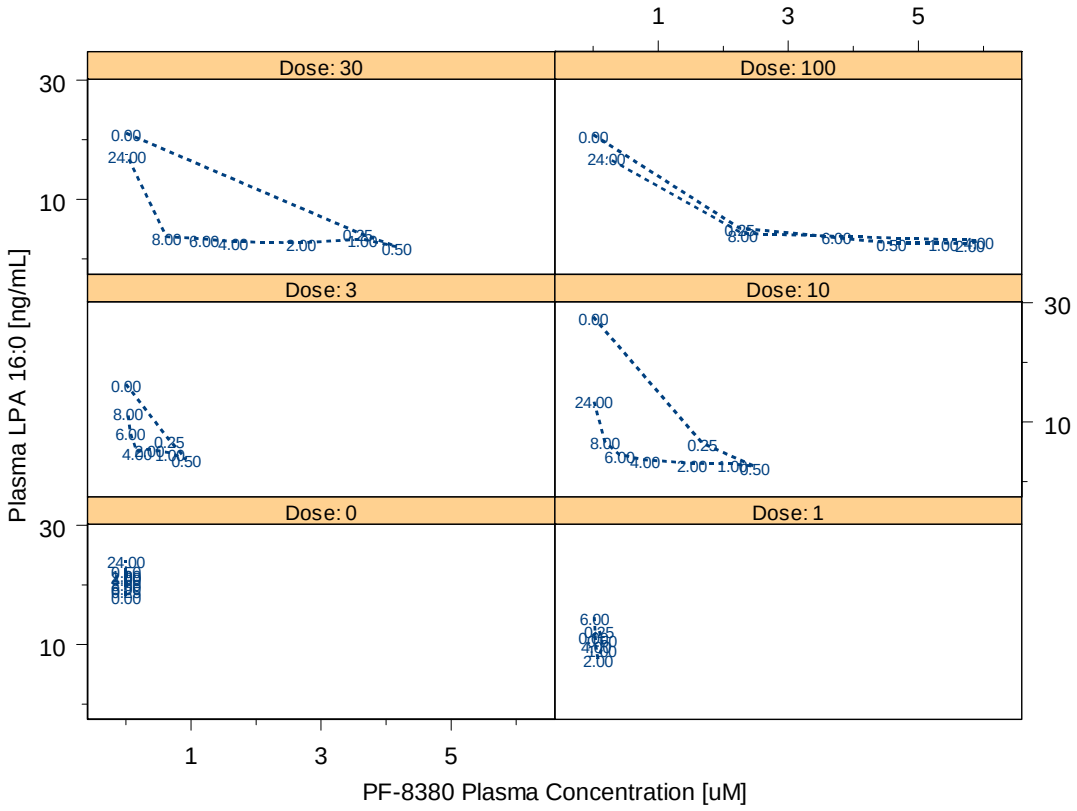

A Novel Autotaxin Inhibitor Reduces Lysophosphatidic Acid Levels in Plasma and the Site of Inflammation

James Gierse*, Atli Thorarensen, Konstantine Beltey, Erica Bradshaw-Pierce, Luz Cortes-Burgos, Troii Hall, Amy Johnston, Michael Murphy, Olga Nemirovskiy, Shinji Ogawa, Lyle Pegg, Matthew Pelc, Michael Prinsen, Mark Schnute, Jay Wendling, Steve Wene, Robin Weinberg, Arthur Wittwer, Ben Zweifel and Jaime Masferrer

Figure S3. C18:0 LPA concentrations as a function of plasma PF-8380 concentration for doses ranging from 0-100 mg/kg. Data points on the graphs are the corresponding blood collection time points.

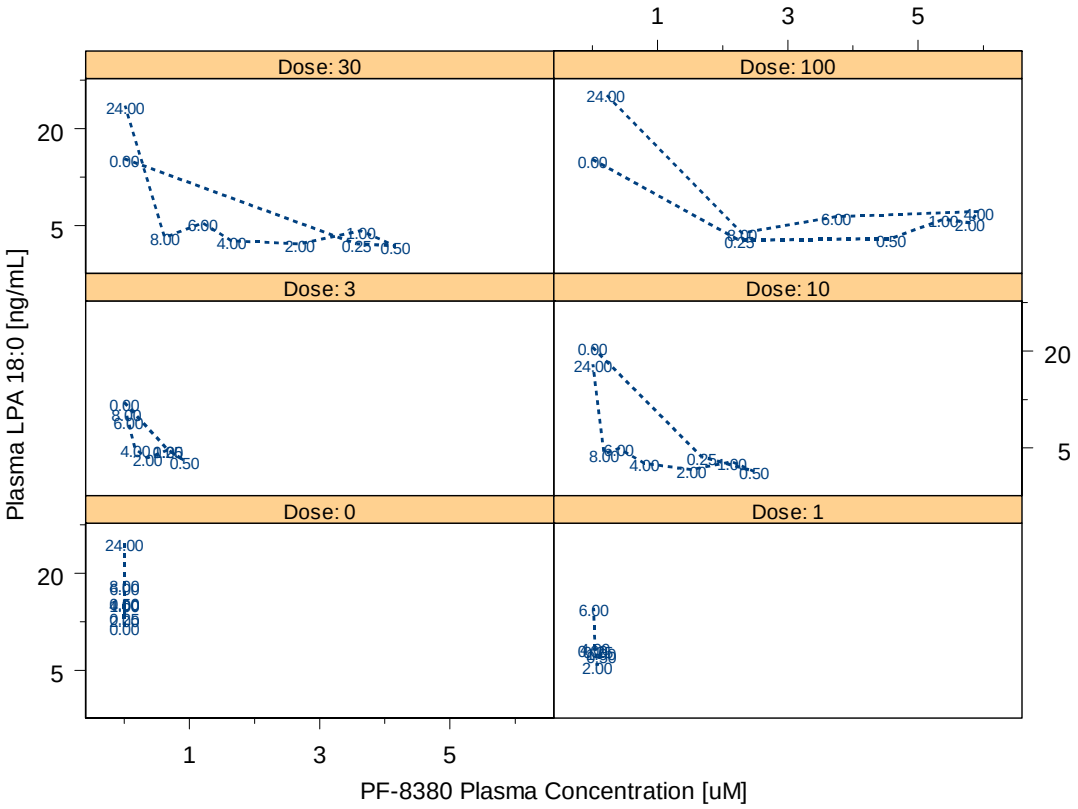

A Novel Autotaxin Inhibitor Reduces Lysophosphatidic Acid Levels in Plasma and the Site of Inflammation

James Gierse*, Atli Thorarensen, Konstantine Beltey, Erica Bradshaw-Pierce, Luz Cortes-Burgos, Troii Hall, Amy Johnston, Michael Murphy, Olga Nemirovskiy, Shinji Ogawa, Lyle Pegg, Matthew Pelc, Michael Prinsen, Mark Schnute, Jay Wendling, Steve Wene, Robin Weinberg, Arthur Wittwer, Ben Zweifel and Jaime Masferrer

Figure S4. C20:0 LPA concentrations as a function of plasma PF-8380 concentration for doses ranging from 0-100 mg/kg. Data points on the graphs are the corresponding blood collection time points.